Electronic properties of self-assembled monolayers on Au(111) studied by electrical force spectroscopy

F. Müller and A.-D. Müller
Institute of Physics, Chemnitz University of Technology, D-09107 Chemnitz, Germany

G. Schmid
Institute of Inorganic Chemistry, University of Essen, 45117 Essen, Germany

(Received 7 November 2000; published 16 April 2001)

Localized voltage dependent capacitive currents through different self-assembled monolayers on Au(111) surfaces were studied by a spectroscopic method in a modified atomic force microscope that detects surface potentials and $\partial C/\partial z$ data as functions of an applied modulated and biased voltage between tip and sample. On flame-annealed Au surfaces, the $\partial C/\partial z$ signal is completely voltage independent. The signal amplitudes on 2-amino-alkanethiol layers change with both ac and dc voltage. The $\partial C/\partial z(U_{dc})$ data obtained represent the energy-dependent density of states of the investigated surface layer. Moreover, the charges of ligand stabilized clusters and the dependence of the clusters' electrical properties on their size were reproduced. The results are discussed in connection with schematic energy models and replacement circuits.

DOI: 10.1103/PhysRevB.63.205403 PACS number(s): 68.18.−g, 07.79.Lh, 73.61.At

I. INTRODUCTION

The density of states (DOS) of organic molecules adsorbed on various well defined surfaces has been a widely studied subject over recent decades.[1] The structure and electronic properties of self-assembled monolayers (SAM's) have been thoroughly investigated by scanning tunneling microscopy STM and atomic force microscopy AFM for an extensive number of molecules,[2] for example, alkanethiols[3,4] and xylylthiols.[5] Chemically deposited clusters on SAM's made of various metals and semiconductors in different sizes[6,7] were utilized to prepare samples for the investigation of single electron tunneling processes such as Coulomb blockade and Coulomb staircase effects.[8–11] In Ref. 12, the DOS of naked gold clusters was numerically calculated as a function of the cluster size. Among the icosahedral gold clusters, the Au_{55} cluster is the smallest one with a nonnegligible density of states at the Fermi energy E_F. It is unknown how the DOS of the cluster changes if it is surrounded by a ligand shell.

In this work, we report with the example of three different SAM's how electrical force spectroscopy in dynamic noncontact AFM can be used to describe their electronic behavior. This investigation might contribute to the comprehension of the conductivity of molecules, for instance 2-amino-alkanethiols, whose chain-length-dependent adsorption structures on Au(111) were investigated in Ref. 3 and whose contact potential differences were observed in Ref. 13. Furthermore, this method is an additional approach to investigating the electronic structure of ligand stabilized clusters.

The article is organized as follows. In Sec. II, the basics for the detection of independent electrical signals in noncontact AFM are briefly considered. The sample preparation is described in Sec. III. The experimental results obtained on several samples are presented and qualitatively discussed in connection with the expectations derived from model descriptions in Sec. IV.

II. ELECTRICAL FORCE SPECTROSCOPY

Electrical force microscopy[14] (EFM) utilizes an atomic force microscope running in dynamic noncontact mode. An additional alternating voltage is applied between tip and sample and causes a small additional force on the cantilever. Due to the nonlinear dependence of the force on the voltage, two additional electrical signals can be detected. In Ref. 15, this method was used to generate simultaneously three images of a surface. In Ref. 16, a lateral resolution of less than 10 nm was achieved with this type of EFM. The method is very similar to kelvin force microscopy (KFM), which was suggested by Nonnenmacher *et al.*[17] In contrast to KFM, in EFM the detected oscillation amplitude at the electrical excitation frequency is not controlled to zero by an external bias voltage.

In noncontact EFM, the lowest mechanical resonance f_r is utilized to control the tip-sample distance. The additional electrical excitation at f_c is realized by applying a U_{dc}-biased alternating voltage with amplitude U_{ac} between tip and sample. Both frequencies f_c and its second harmonic $2f_c$ are lower than f_r. The detected signal amplitudes of the cantilever vibration X_f and X_{2f} at f_c and $2f_c$, respectively, are given by

$$X_f \propto -\frac{\partial C(U_{dc})}{\partial z} U_{dc} U_{ac} \tag{1}$$

and

$$X_{2f} \propto \frac{\partial C(U_{dc})}{\partial z} \frac{U_{ac}^2}{4}. \tag{2}$$

Both are proportional to the derivative of the tip-sample capacitance with respect to the distance $[\partial C(U_{dc})/\partial z]$. In most tip-sample geometries, $\partial C/\partial z$ is proportional to the tip-sample capacitance $C(U_{dc})$ itself. Additionally, X_f depends linearly on the potential difference U_{dc} between tip and

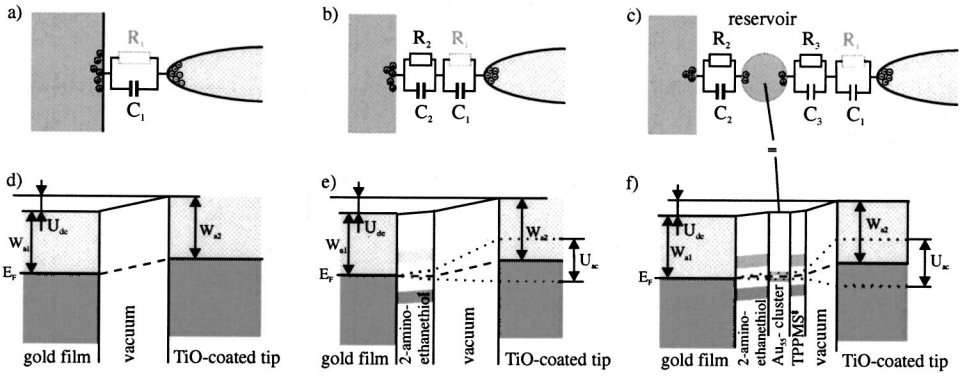

FIG. 1. Replacement circuits (a)–(c) and energy diagrams (d)–(f) of different tip-sample geometries. (a) and (d), metallic sample. (b) and (e), metallic sample with nonmetallic layer (for instance, self-assembled monolayers of 2-amino-ethanethiol). (c) and (f), ligand stabilized metal clusters [for instance, Au_{55} clusters stabilized with $(C_6H_5)_2P(C_6H_4SO_3Na)_3$ (TPPMS)] connected by an organic molecule to the metallic substrate.

sample. The applied voltage U_{dc} at which X_f becomes zero is given by the work function difference between tip and sample,[15]

$$U_{dc}|_{X_f=0} = U_K = -\frac{\Delta W_a}{e}, \tag{3}$$

if there are no additional voltage sources in the system. In order to detect the electrical signals, two lock-in amplifiers (Stanford Research SR 830) with small bandpasses at f_c and $2f_c$ were used. As probe tips, V-shaped TiO-coated silicon cantilevers (MikroMasch^{TM}) with a force constant of 4 N/m and resonance frequencies of approx. 30 kHz were mounted in a Discoverer^{TM} AFM (TopoMetrix Inc.). The connections for the evaluation of the electrical signals are not commercial. In spectroscopy mode, U_{dc} is swept while the signals X_f and X_{2f} are recorded for several modulation amplitudes U_{ac}. From the $X_f(U_{dc})$ data, the work function difference between tip and sample is determined. The information about $\partial C/\partial z$ is extracted from the $X_{2f}(U_{dc})$ data, because X_{2f} is independent of U_{dc}.

III. SAMPLE PREPARATION

A. Au(111)

From the literature, various preparation procedures are known for an atomically flat Au(111) surface, e.g., stripping of mica[18,19] or flame annealing of evaporated gold films on glass.[4] For the present experiments, the flame annealing method was used. A borosilicate glass was prepared by rinsing in ethanol and short (about 1 min) etching in 10% HF solution to increase the adhesion of the 3 nm Cr layer (1 nm/min). This Cr layer and a 100 nm gold film (30 nm/min) were prepared by thermal evaporation in a high-vacuum HV chamber. It proved advantageous to mount the substrates on top of a metal grating about 10 cm above the evaporator ship. In this way, the condensation heat is conducted through the metal grating instead of the glass substrate. In order to obtain an atomically flat Au(111) surface, the sample was annealed in a reducing butane flame until red heat and quickly cooled down.

B. Adsorbate layers on Au(111)

For the adsorption of organic molecules or layers of ligand stabilized clusters, two preparation methods are known. They differ from each other in the adsorption rate. The fast method increases the adsorption rate by heating[4] or improving the mobility with ultrasound. This special process of gold cluster adsorption is described in Ref. 9. The slow method was used, for instance, in Ref. 20. Therein, the samples are stored for several hours in the adsorbent solution and thoroughly rinsed in the solvent. Analogously, our samples were prepared by dipping the substrate for 24 h in a $10^{-3}M$ 2-amino-ethanethiol solution and rinsing in ethanol. The adsorption of the ligand stabilized Au_{55} clusters[21] needs further soaking for 24 h in a $10^{-6}M$ aqueous cluster solution and rinsing in water. The Pt_{309} cluster covered samples were prepared by soaking the 2-amino-ethanethiol covered Au(111) for 18 h in an ethanolic solution of Pt_{309} clusters and rinsing in ethanol. The composition of the clusters is $Au_{55}(Ph_2PC_4H_6SO_3Na)_{12}Cl_6$ (Ph is phenyl) and $Pt_{309}SO_3H$, respectively.

IV. EXPERIMENTAL RESULTS

In the experiments, we acquired a complete set of $X_f(U_{dc})$ data and $X_{2f}(U_{dc})$ data with U_{ac} as parameter. The single characteristics were very reproducible and show almost no noise. In the following, the $X_{2f}(U_{dc})$ data on several samples will be compared and discussed by means of the schematic energy diagrams and replacement circuits in Fig. 1.

A. Au(111)—a metallic sample

This investigation was done to confirm the substrate's properties: monatomic flat terraces of a chemically clean Au(111) surface. In the AFM under ambient conditions, such terraces with different lateral dimensions have been found. Because of surface contamination in air and diffusion, the atomic structure of Au(111) is only stable for several hours.

When the tip and sample are metallic, the tip-sample geometry can be modeled by an Ohmic resistance $R(U)$ and a

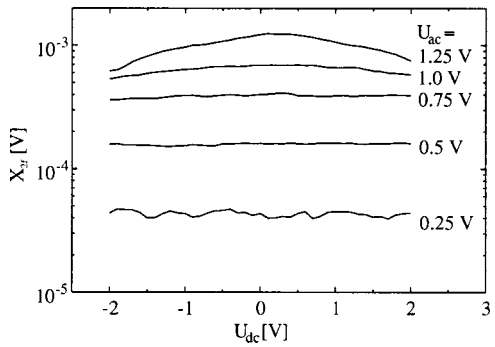

FIG. 2. $X_{2f}(U_{dc})$ data for different alternating voltage amplitudes U_{ac} detected on a Au(111) surface 20 min after preparation.

parallel circuited impedance $1/\omega C(U)$. The corresponding schematic model and energy diagram are drawn in Figs. 1(a) and 1(d), respectively. Due to the very high carrier concentration and carrier mobility in metals, the capacitance C_1 depends only on the tip-sample geometry. Consequently $\partial C/\partial z$ is independent of the voltage amplitude U_{ac} as well as of U_{dc}. Thus, X_{2f} should be independent of U_{dc} and proportional to U_{ac}^2.

Combined tunneling current and force measurements have shown that a significant tunneling current flows only in the repulsive part of the force-distance curve.[22] In our experiments, no tunneling current was detectable. Therefore, R_1 approaches infinity, and the dc current through R_1 is negligible.

The set of $X_{2f}(U_{dc})$ data plotted in Fig. 2 was detected about 20 min after flame annealing. For $U_{ac} \leqslant 1$ V, the expected independence of U_{dc} was found. For larger amplitudes, a square dependence of X_{2f} on U_{dc} might be observed. The effective tip-sample distance is influenced by the increased electrical static force, which is proportional to $(U_{dc}^2 + U_{ac}^2/2)$.[23]

In the $X_f(U_{dc})$ data, a U_K of about 155 ± 30 mV can be estimated. The values of X_{2f} at U_K for different U_{ac} can be used to verify the quadratic dependence of X_{2f} on U_{ac}. In Fig. 3, these values are drawn together with a second order polynomial fit. The good agreement of data and fit proves Eq. (2).

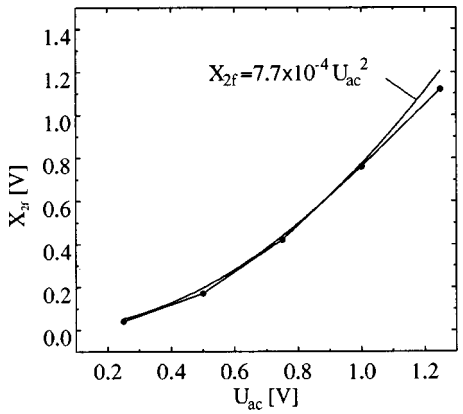

FIG. 3. Comparison between the $X_{2f}(U_{ac})$ data extracted from the measurement in Fig. 2 and a fit that is proportional to U_{ac}^2.

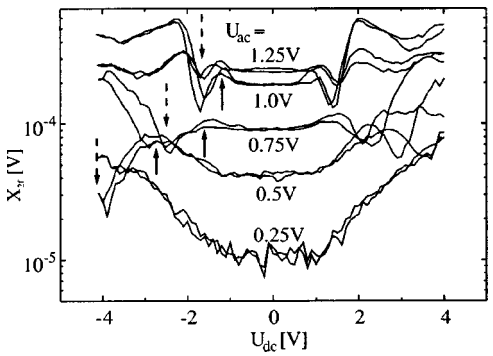

FIG. 4. $X_{2f}(U_{dc})$ data for several U_{ac} detected on a 2-amino-ethanethiol layer on Au(111).

B. 2-amino-ethanethiol on Au(111)

Thin surface layers on a metallic substrate can be described as a series of two capacitances C_1 and C_2, each of them parallel to an Ohmic resistance R_1 and R_2 as shown in Figs. 1(b) and 1(e). The index 2 corresponds to the surface layer itself, while the index 1 matches the vacuum gap between surface and tip. As discussed for the metal sample, R_1 approaches infinity. Thus, the dc voltage drops mainly over R_1.

For a thin (mono)molecular film, the capacitance C_2 is larger than C_1, and the ac voltage drops mainly over the smaller capacitance C_1. This is plotted in Fig. 1(e), where the dotted (ac) and dashed (dc) lines show the related potential decays. The remaining voltage $\overline{U_2}$ at the layer surface can be expressed as kU_{dc} with $k<1$.

For the investigated self-assembled 2-amino-ethanethiol on Au(111), U_K was about -90 mV. A set of $X_{2f}(U_{dc})$ data is shown in Fig. 4. The shapes of these curves differ generally from the characteristics on Au(111). The absolute signal amplitude at U_K is about four times lower than on gold. With increasing U_{ac} the curves are compressed horizontally (k increases). The capacitance maxima marked with solid arrows shift from -2.8 V ($U_{dc}=0.5$ V) to -1.2 V ($U_{dc}=1.0$ V). Simultaneously, the capacitance minima (dashed arrows) shift from about -4 V to -1.5 V.

The $X_{2f}(U_{dc})$ data represent approximately the carrier density distribution in the surface layer at the energy $E = E_F + e\overline{U_2}$, while $\overline{U_2}$ is a function of U_{dc} and U_{ac}. From corresponding points in data taken with different U_{ac}, a linear growth of $\overline{U_2}$ with increasing U_{ac} can be derived. This means that k also increases linearly with increasing U_{ac} within this voltage range.

Between $U_{ac}=1$ V and $U_{ac}=1.25$ V no further compression occurs. These two characteristics differs from each other only by the averaged signal amplitude, i.e., k does not increase further with increasing U_{ac}.

C. Chemically bound Pt_{309} clusters and Au_{55} clusters on Au(111)

The additional adsorption of ligand stabilized clusters will result in the case that is drawn in the Figs. 1(c) and 1(f). Due to the ligand shell around the clusters, two organic layers

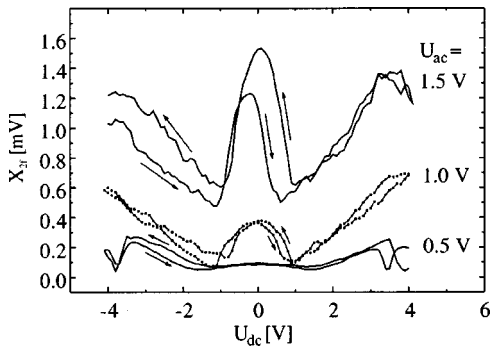

FIG. 5. $X_{2f}(U_{dc})$ data for several U_{ac} detected on a layer of Pt_{309} clusters on 2-amino-ethanethiol as spacer molecules.

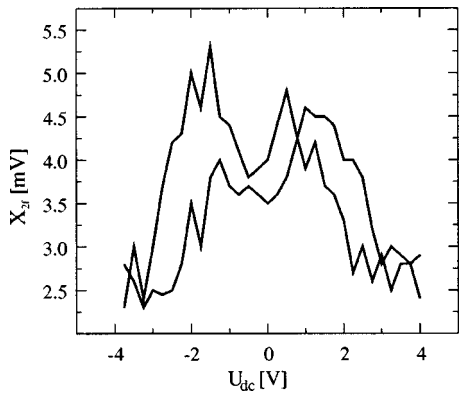

FIG. 6. $X_{2f}(U_{dc})$ data for $U_{ac}=1$ V detected on a layer of TPPMS stabilized Au_{55} clusters with 2-amino-ethanethiol as spacer molecules.

have to be considered. One corresponds to the spacer molecule together with the ligand shell (R_2 and C_2) and the other to the ligand shell in the tip direction (R_3 and C_3). This model is very similar to the model used in Ref. 8.

The cluster acts as a carrier reservoir. It depends on the cluster size as well as on the electric field $\overline{E}$ whether or not the cluster states can be detected with $X_{2f}(U_{dc})$ spectroscopy. For small $\overline{E}$, a small cluster contains enough carriers to compensate charges. An increase of $\overline{E}$ causes the $X_{2f}(U_{dc})$ data to reflect the energy-dependent density of states inside the cluster as long as the cluster is large enough. If the cluster is too small, more spacer properties will be reproduced in the $X_{2f}(U_{dc})$ data.

The results for Pt_{309} clusters were obtained within the first 15 min after preparation. This is shown in Fig. 5. One notes that the outline of the characteristics is less dependent on U_{ac} than the $X_{2f}(U_{dc})$ data in Fig. 4. Using the model from Fig. 1(c), one can conclude that the relation between R_2 and (R_1+R_3) is approximately independent of U_{ac}. This is only possible if the cluster contains enough free carriers to provide the necessary current. k is almost constant. One detects two minima at $U_{dc}=-1.2$ V± 0.35 V and $U_{dc}=1.0$ V ± 0.35 V. Uniformly for all U_{ac} the signals around E_F are higher than away from E_F.

U_K varies between -400 mV and 80 mV. Comparing data taken in different sweep directions, a charging of the cluster compared to the substrate can be observed. If the sweep starts at negative tip voltages, the cluster is negatively charged compared to the sample. Its energetic position is shifted to positive potentials. If the discharging is slower than the tip potential sweep, the cluster is still negatively charged if the tip potential crosses $U_{dc}=0$ V. The maximum signal is detected at $U_{dc}=-0.3$ V for all U_{ac}. Starting at positive voltages, the same maximum is found at $U_{dc}=0.05$ V. A dependence of this charging effect on U_{ac} has not been found.

In comparison to the large Pt_{309} clusters, Au_{55} clusters show a completely different behavior. Figure 6 shows $X_{2f}(U_{dc})$ data detected with $U_{ac}=1$ V on TPPMS stabilized Au_{55} clusters on 2-amino-ethanethiol. The signal at $U_{dc}=0$ V is smaller than at voltages around ± 1.5 V and higher than for $|U_{dc}|\geqslant 2.5$ V. One can conclude that the ligand stabilized Au_{55} clusters have a lower density of states at the Fermi energy than away from the Fermi energy.

In summary, spectroscopy of the electrical signals in the AFM seems to be suitable to investigate the local electronic properties of surfaces as known from scanning tunneling spectroscopy. The discussion with comparison to several energy diagrams shows that the dc-voltage-dependent characteristics should be an indirect measure of the energy-dependent density of states in self-assembled monolayers. Due to the distance-dependent ratio between tip-surface resistance and layer resistance, the exact energy scale cannot be obtained. On 2-amino-alkanethiol layers, the scaling factor between the applied voltage U_{dc} and the spectroscopy level $\overline{U_2}$ increases with increasing U_{ac} as long as U_{ac} does not exceed 1 V.

The additional adsorption of ligand stabilized clusters leads to a sample type that has been thoroughly investigated by STM previously. There, the cluster acts as a further carrier reservoir in a double barrier system. In electrical force spectroscopy, the electrical properties of the cluster itself influence the detected $X_{2f}(U_{dc})$ data. The two tested cluster types (Pt_{309} and Au_{55}) show different behavior around the Fermi energy E_F. The smaller Au_{55} clusters have a decreased DOS around E_F, while the DOS of Pt_{309} is increased at E_F in relation to states away from E_F.

ACKNOWLEDGMENTS

Two authors of this work (F.M. and A.-D.M.) were supported by the Deutsche Forschungsgemeinschaft (INK 2/B3 and Graduiertenkolleg ''Thin Films and Non-Crystalline Materials''). This is gratefully acknowledged, as is the scientific cooperation with the members of Professor Schmid's group.

[1] W. Göpel, Ch. Ziegler, *Nanostructures Based on Molecular Materials* (VCH, New York, 1992).
[2] *Clusters and Colloids. From Theory to Applications*, edited by G. Schmid (VCH, Weinheim, 1994).
[3] J. Voets, J.W. Gerritsen, R.F.P. Grimbergen, and H. van Kempen, Surf. Sci. **399**, 316 (1998).
[4] S. Xu, S.J.N. Cruchon-Dupeyrat, J.C. Garno, G.-Y. Liu, G.K. Jennings, T.-H. Yong, and P.E. Laibinis, J. Chem. Phys. **108**, 5002 (1998).
[5] S. Datta, W. Tian, S. Hong, R. Reifenberger, J.I. Henderson, and C.P. Kubiak, Phys. Rev. Lett. **79**, 2530 (1997).
[6] M.P.J. van Staveren, H.B. Brom, L.J. de Jongh, and G. Schmid, Solid State Commun. **319**, 60 (1986).
[7] K. Puech, F. Henari, W. Blau, D. Duff, and G. Schmid, Europhys. Lett. **119**, 32 (1995).
[8] R.P. Andres, T. Bein, M. Dorogo, S. Feng, J.I. Henderson, C.P. Kubiak, W. Mahoney, R.G. Osifchin, and R. Reifenberger, Science **272**, 1323 (1996).
[9] M. Dorogi, J. Gomez, R. Osifchin, R.P. Andres, and R. Reifenberger, Phys. Rev. B **52**, 9071 (1995).
[10] R. Houberts, T. Feigenspan, F. Mielke, U. Memmert, U. Hartmann, U. Simon, G. Schön, and G. Schmid, J. Vac. Sci. Technol. B **9**, 814 (1991).
[11] J.A. Reedijk, L.J. Adriaanse, H.B. Brom, L.J. de Jongh, and G. Schmid, Phys. Rev. B **57**, R15 116 (1998).
[12] O.D. Häberlain, S.-C. Chung, M. Stener, and N. Rösch, J. Chem. Phys. **106**, 5189 (1997).
[13] R.C. Thomas, P. Tangyunyong, J.E. Housten, T.A. Michalske, and R.M. Crooks, J. Phys. Chem. **98**, 4493 (1994).
[14] D. Sarid, *Atomic Force Microscopy* (Oxford University Press, Oxford, 1991).
[15] F. Müller, A.-D. Müller, M. Hietschold, and S. Kämmer, Microelectron. Reliab. **37**, 1631 (1997).
[16] A.-D. Müller, F. Müller, M. Kröll, and G. Schmid, Appl. Surf. Sci. **171**, 125 (2001).
[17] M. Nonnemacher, M.P. O'Boyle, and H.K. Wickramasinghe, Appl. Phys. Lett. **58**, 2921 (1991).
[18] M. Hegner, P. Wagner, and G. Semenza, Surf. Sci. **291**, 39 (1993).
[19] P. Wagner, M. Hegner, H.-J. Güntherodt, and G. Semenza, Langmuir **11**, 3867 (1995).
[20] S. Peschel and G. Schmid, Angew. Chem. Int. Ed. Engl. **107**, 1568 (1995).
[21] G. Schmid, R. Boese, R. Pfeil, F. Bandermann, S. Meyer, G.H.M. Calis, and J.W.A. van der Velden, Chem. Ber. **114**, 3634 (1981).
[22] M. Specht, F. Ohnesorge, and M. Heckl, Surf. Sci. Lett. **257**, L635 (1991).
[23] F. Müller, A.-D. Müller, and M. Hietschold, Meas. Sci. Technol. **9**, 734 (1998).